

Letter of Intent
December, 2005

**Measurement of $\Delta\sigma^{\gamma N}(k)$ and the High
Energy Contribution to the Gerasimov-Drell-Hearn Sum Rule**

Yelena Prok (contact: yprok@jlab.org)
Massachusetts Institute of Technology

Peter Bosted
Jefferson Lab

Donald Crabb
University of Virginia

Daniel I. Sober
The Catholic University of America

Abstract

We propose to measure the spin-dependent total cross section for circularly polarized photons absorbed on longitudinally polarized protons and neutrons in the photon energy range $2.5 < k < 5.5$ GeV. This will be the first measurement of the difference between left- and right-handed polarized photoproduction above the resonance region. These data are needed to learn about the high energy convergence of the fundamental Gerasimov-Drell-Hearn sum rule for the proton and neutron. Substantial contributions are expected in this energy range, especially for the isovector combination. Measurements of the magnitude and energy-dependence of polarized photoabsorption at high energy will provide the baseline for understanding of soft Regge physics, essential to the interpretation of data taken with virtual photons. The results can be compared with the variety of models based on Reggeon and Pomeron exchange. We propose to use the frozen spin target, circularly polarized tagged photon beam and CLAS detector in Hall B. The proposed experiment will be an extension of an already approved experiment [35] at beam energies up to 2.3 GeV. We request 15 days of running time, with 5 days of data taking with the polarized proton target and 10 days of data taking with the polarized deuteron target.

1 Introduction and Motivation

1.1 The GDH Sum Rule

The Gerasimov-Drell-Hearn (GDH) sum rule [1] is one of the most fundamental relations in hadronic physics, and its experimental test is one of the major challenges for photoproduction experiments over the next decade. The GDH sum rule relates the difference in total hadronic photo-absorption cross sections for left- ($\sigma_A^{\gamma N}$) and right-handed ($\sigma_P^{\gamma N}$) circularly polarized photons interacting with longitudinally polarized nucleons to the square of the nucleon's anomalous magnetic moment κ ,

$$\int_{k_\pi}^{\infty} \frac{dk}{k} \Delta\sigma^{\gamma N}(k) = \frac{2\pi^2 \alpha \kappa^2}{M^2} \quad (1)$$

where k is the photon energy, $\Delta\sigma^{\gamma N}(k) = \sigma_P^{\gamma N}(k) - \sigma_A^{\gamma N}(k)$, M is the nucleon mass, and the threshold energy k_π needed to produce at least one pion is about 0.15 GeV. An alternate notation is $\Delta\sigma^{\gamma N} = \sigma_{3/2}^{\gamma N} - \sigma_{1/2}^{\gamma N}$, where 1/2 (3/2) refers to the spin of the nucleon-photon system. Note that we have chosen a definition of $\Delta\sigma^{\gamma N}(k)$ for which the GDH integral is positive: frequently the opposite sign convention is chosen.

Numerically, the GDH sum rule prediction is 204 μb for the proton, 232 μb for the neutron, and 219 μb (-15 μb) for the average isoscalar (isovector) combinations. The fundamental meaning of the sum rule is that any particle with a non-zero anomalous magnetic moment must have an excitation spectrum and internal structure. The energy scale at which the sum rule is saturated gives an indication of the energy scale beyond which nucleonic excitations become asymptotically spin-independent.

Many authors [2] have analyzed the connection between the GDH sum rule, valid for real photons ($Q^2 = 0$), and the analogous sum rules for virtual photons, in particular the equally fundamental Bjorken Sum Rule [3] for $Q^2 \rightarrow \infty$, which has been the subject of intense experimental study in the past decade. A generalized GDH Sum Rule can be formed that smoothly connects the $Q^2 = 0$ and large Q^2 limits. These 'end points' measurements of total cross section helicity asymmetry would complement the numerous virtual photon measurements for the analogous Bjorken Sum Rule. Data from this proposal will compliment the vast body of spin-averaged data on $\sigma^{\gamma N}(k)$. Measurements of the spin degree of freedom will help to gain insight into underlying reaction mechanism for photo-absorption, such as the role of reggeon exchange and a possible pomeron cut contribution. A good understanding of soft Regge physics is essential for the interpretation of the Q^2 -dependence of data taken with virtual photons.

1.2 Energy Dependence of $\Delta\sigma^{\gamma N}$

Based on the $1/k$ factor in the GDH integral, combined with the expectation of a strong spin dependence in the excitation of the dominant nucleon resonances (for example, $\sigma_{1/2}^{\gamma N} \approx (1/3)\sigma_{3/2}^{\gamma N}$ for the prominent $\Delta(1232)$ resonance), one would guess that the GDH integral would be saturated at photon energies of about 1.7 GeV, the traditional cutoff between the

resonance region and deep inelastic scattering. Multipole analyses [4] of unpolarized pion photoproduction data suggest that for the proton or neutron individually, the resonance region contributions are about 20% above (for the proton) or below (for the neutron) the sum rule values, with substantial contributions possible at higher energies. In the isovector case (difference of proton and neutron), the contributions from major resonances such as the $\Delta(1236)$ cancel, with principally *non-resonant* contributions at low energy, and equally large contributions at high energy.

As summarized by [5], the resonance region multipole analyses give integral values of 257 to 289 μb for the proton (well above the GDH integral), and 169 to 189 μb for the neutron (well below the GDH integral). Looked at another way, the resonance region would seem to account for most of the *isoscalar* $[(p+n)/2]$ strength, but gives contributions of 34 to 65 μb for the *isovector* $[(p-n)/2]$ combination, compared to the GDH value of -15 μb . We can therefore deduce that the integrated strength above the resonance region should be quite large (of order 25 to 50 μb) for both proton and neutron, but of opposite sign.

Regge theory gives a good description of many processes, and thus should be a reasonable guide to the high energy behavior of $\Delta\sigma^{\gamma N}$. In this framework, the energy dependence for a given Regge trajectory is given by s^{α^0-1} , where $s = M^2 + 2Mk$ is the squared total center of mass energy, and α^0 is the intercept, which is related to the spin J , mass m_r , and intercept slope α' (of order $0.8 - 0.9 \text{ GeV}^{-2}$) by $\alpha^0 = J - \alpha'm_r^2$. As discussed in some detail in [5, 6], the isovector contribution to $\Delta\sigma^{\gamma N}$ is expected to be dominated by the poorly known $a_1(1260)$ axial vector meson trajectory (α^0 is generally thought to be in the range -0.5 to 0), while the isoscalar contributions are expected to be dominated by the better known $f_1(1285)$ meson trajectory (α^0 of -0.4 ± 0.1). Contributions from higher mass trajectories could also be important. In addition, both [6] and [5] consider possible isoscalar contributions from non-perturbative gluon exchange (proportional to $\ln s/s$) as suggested by [7]. Finally, [6] also considers a possible two-pomeron cut contribution (proportional to $1/\ln s^2$).

1.3 Connection to Virtual Photo-absorption

Bianchi and Thomas [5] have shown that extending their Regge parameterization to $Q^2 > 0$ can give a quite reasonable description of all available deep inelastic data for the spin structure function g_1 , covering a wide range of x and Q^2 . They made three different fits, with slight variations in some of the assumptions, and all of them give a $\chi^2/\text{d.f.}$ as good as NLO pQCD fits based on polarized quark and gluon distribution functions. This shows the duality between different ways of describing hadronic physics. From our point of view, the big advantage of the Regge theory is that it allows a prediction of $\Delta\sigma^{\gamma N}(k)$ for real photons. From another point of view, good measurements with real photons might help to understand the high energy (low- x) behavior of g_1 , especially if the $(\ln s)/s$ or pomeron-pomeron cut contributions are larger than expected [6]. There is a considerable uncertainty in extrapolating the data on g_1 to $x = 0$. This is currently the largest uncertainty in testing the Bjorken and Ellis-Jaffe sum rules, which both involve integrals of g_1 over the range $0 < x < 1$. Especially in the neutron case, the $\chi^2/\text{d.f.}$ for fits that give a divergent integral

are only slightly worse than fits that give a convergent integral. It will be very interesting to measure the analogous cross sections with real photons.

1.4 Experimental status

For reliable determinations of $\Delta\sigma^{\gamma N}$, it is essential to make direct measurements of the total cross section difference using polarized photons and polarized targets. Experimentally, the GDH integrand is determined from the resonance region up to the onset of the Regge regime. The resonance region contributions up to about $k = 3$ GeV have recently been measured at MAMI and ELSA. The latest measurements on the proton have been performed at MAMI [37] in the energy range of 0.14 to 0.8 GeV, and at ELSA [36] in the energy range of 0.7 to 3.0 GeV. The measurement on the deuterium target have been also performed at both facilities, with the beam energy up to 800 MeV at MAMI, and 1.8 GeV at ELSA. Both experiments used tagged photons, and a frozen spin target inside of a large acceptance detector. Evaluations of the GDH integrand using preliminary results from MAMI and ELSA have appeared in conference proceedings. The value of the GDH sum rule for the proton up to 2.9 GeV is quoted as $226 \pm 5_{stat} \pm 12_{syst} \mu b$, while the prediction for the proton is $205 \mu b$ [36]. To determine the full integral, theoretical estimates must be used for the lower and higher unmeasured energy regions. The integral above 2.9 GeV is predicted by a recent phenomenological analysis by Bianchi and Thomas [5] which uses a Regge parametrization of polarized deep inelastic lepton scattering data to predict the multi-pion contributions to the GDH sum rule at $Q^2 = 0$, and is $-15 \mu b$.

For the sum rule to be satisfied, the integral above 2.9 GeV must be $-21 \mu b$, which is consistent with the Bianchi and Thomas parametrization. The E159 experiment planned at SLAC to measure the integral in the energy range of 4 to 40 GeV has been unfortunately put on indefinite hold, but there exists a possibility of measuring the integral up to 6 GeV at Jefferson Lab. The estimate for the GDH integral on the neutron is $255 \mu b$ while the Sum Rule prediction is $233 \mu b$. Particularly interesting is the iso-vector case (proton-neutron). The estimate for the total integral is $-43 \mu b$, compared with the Sum Rule prediction of $-23 \mu b$. The estimate shows a near cancellation of the proton and neutron contributions in the resonance region, and most of the strength in the iso-vector case coming from the higher energies. To fully test the GDH sum rule, the high energy behavior must be determined for both proton and neutron targets, in order to test the isoscalar and isovector sum rules separately.

A 3-day test run was performed at Jlab in 2001, where the helicity asymmetry of the γp cross section was measured using tagged photon beam and a solid polarized $^{15}NH_3$ target in Hall B. Neither the target nor the beam line were optimized for photon running, so the trigger rate was dominated by accidental coincidences between the tagging system and the CLAS detector. The quality of photon beam was very poor during this run, with the photons not collimated and scraping the beam pipe, producing showers that dominated the trigger. Due to the high accidental rate, all-neutral events from this run could not be reliably identified, and therefore excluded from analysis. Accepted events were required to contain at least one charged particle track in the drift chambers. The tracks were projected

back to the beam line, and events not pointing back to the target cell were rejected. The asymmetry was calculated for each sign of target polarization, and combined to give a single value for each energy bin. Using the Particle Data Group’s parametrization of the total γp cross section [39], the measured events with charged-particle tracks were estimated to constitute about 50% of the total cross section [34]. Assuming that the unmeasured part of the total cross section has the same helicity as the measured part, the contribution to the GDH sum rule at energies of 2.5 to 5.5 GeV can be calculated. The results are shown in Fig. 1, along with the 3 model predictions of Bianchi and Thomas [5]. Model 2 is the author’s best fit to electron scattering data, while Models 1 and 3 have some limiting assumptions. An accurate estimation of the total cross section from this experiment was not possible,

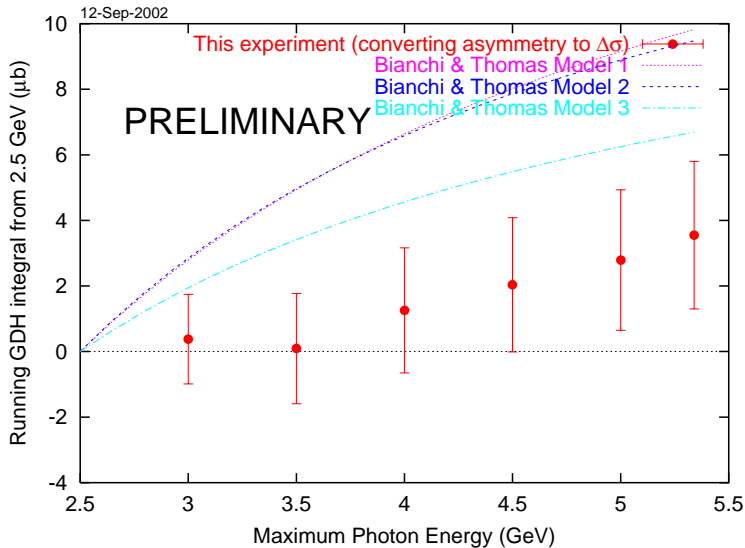


Figure 1: Running GDH integral beginning at 2.5 GeV. Data points: 3-day real photon run in January of 2001, using PDG parametrization.

but the data has shown the existence of an interesting structure of the helicity asymmetry for the photon energy range of 2.5-5.5 GeV.

1.5 How to measure $\Delta\sigma^{\gamma N}(k)$ for the neutron

We plan to measure $\Delta\sigma^{\gamma N}(k)$ for the neutron by using both proton and deuteron targets, and making small corrections to the approximation that the deuteron is the average of proton and neutron cross sections. As we did for virtual photons, we will take into account the approximately 5% D-state probability in the deuteron wave function. At very low energies there are corrections due to processes such as deuteron photodisintegration near threshold (2.2 MeV) and coherent π^0 production, as well as effects due to final state interactions, meson exchange currents, shadowing, and relativistic effects [9].

2 Experimental Overview

We will use tagged circularly polarized photons produced by the bremsstrahlung of longitudinally polarized electrons. The polarization of the electron beam will be monitored by the Hall B Møller polarimeter. For targets, we will use polarized $C_4H_9(OH)$ and $C_4^2H_9(O^2H)$ as sources of polarized protons and neutrons. The target will be surrounded by the start counter scintillators which are normally used for photon running because of the long flight times from the target to the detector. Details of the photon beam, target, detector, and expected experimental sensitivity are given in the next sections. The last section summarizes our request for beam time.

2.1 Photon Beam

We will employ circularly polarized photons produced by bremsstrahlung off longitudinally polarized electrons incident on an amorphous radiator. The helicity state of the electron beam will be reversed 30 times per second and encoded in the data acquisition stream. The beam flux in each helicity state can be monitored by a synchrotron light monitor located at the final bend of the electron beamline. The degree of circular polarization of the photon beam depends on the ratio E_γ/E_e , and ranges from 60% to 99% of the incident electron beam polarization P_e for photon energies E_γ between 50% and 95% of the incident electron energy. The circular polarization of the photon beam is given by [32]:

$$P_o = P_e \frac{4x - x^2}{4 - 4x * 3x^2}, \quad (2)$$

where $x = E_\gamma/E_e$. Since the circular polarization of the bremsstrahlung photons can be calculated precisely from the longitudinal polarization of the photon beam, no additional beam polarimetry will be required beyond the standard Hall B Møller polarimeter. The photon beam will be collimated to approximately 1 cm on the 1.5 cm in diameter target. This can be accomplished with the 2.6 mm collimator which exists in Hall B, and has been previously used in the experiments. The collimation will have a small and calculable effect on the circular polarization.

We propose to measure the photon flux at the target through sampling of 'out-of-time' electron hits in the tagger T-counters, as described in CLAS-NOTE [33]. The 'out-of-time' electrons are 'good' electrons detected in the tagger which are not involved in the physics event trigger, where a 'good' electron is detected when the left and right TDC hits of a T-counter match in time along with a matched hit in time for one E-counter.

The total number of 'good' electrons in the tagger hodoscope is compared with the number of photons on the target measured with the total absorption counter (TAC) placed directly in the photon beam. The ratio of these two is defined as the tagging ratio, and, multiplied by the total number of 'good' electrons it gives the total photon flux per T-Counter. The photon flux can be rebinned in fine energy bins by rationing the flux from each T-counter to the desired binning by the fractional amount each desired bin occupies with respect to the T-counter. Electron current for photon tagging is typically in the 5-10 nA range.

2.2 Target

A new frozen-spin target that is being developed at Jefferson Lab will allow the detection of particles in an angular acceptance of 4π , in contrast to the standard solid polarized target which leaves only a small acceptance for emitted particles due to its strong magnetic field and large size of the magnet itself that occupies much of the space around the target cell. The frozen spin target introduces minimum distortion to the trajectories of outgoing charged particles and, and allows to take advantage of large acceptance spectrometers such as CLAS. The disadvantage of such targets is the low cooling power, but since the photon beam introduces very little heat or radiation damage, the target can be used successfully with a tagged photon beam.

The 'frozen spin' technique is based on the long nucleon spin relaxation times at temperatures below 70 mK. The high nucleon polarization obtained via Dynamic Nuclear Polarization, in a high magnetic field and with the use of the microwave irradiation, can be preserved after turning the microwaves off, and reducing the temperature as much as possible. The relaxation time of the sample is a function of B/T , where B is the magnetic holding field, and T is the material temperature. By operating at optimally low temperature, it is possible to preserve high polarization in a holding field of less than 0.5 T for time periods acceptable for running the experiment. The polarization decays exponentially, and needs to be repolarized every few days.

The design of Hall B frozen spin target is similar to the frozen spin target used at Mainz-Bonn GDH experiments [28]. A horizontal $^3\text{He}/^4\text{He}$ dilution refrigerator is a central part of the target. It is used to provide the lowest temperatures, with the typical values of 50 mK for frozen spin operation and 200-500 mK when polarizing. The polarizing magnet is a 5.1 Tesla warm bore solenoid 127 mm in diameter, with field homogeneity of $\frac{\Delta B}{B} < 3 \times 10^{-5}$. The lower holding field is provided by an internal superconducting solenoid, which consists of 3 layers of 0.1 mm in diameter NbTi wire. The solenoid is 50 mm in diameter and 110 mm long, with the maximum field of 0.42 Tesla and field homogeneity of $\frac{\Delta B}{B} < 3 \times 10^{-3}$. The holding field will maintain nucleon polarization longitudinally to the beam and provide the field necessary for the NMR measurements. The transverse holding coil is in its design stage, however, this experiment requires only the longitudinally polarized target. Movement of the refrigerator within CLAS will be required in order to move target from the strong polarizing field to the weaker holding field. Once in the hall, the target operation will consist of two stages [29]: polarization stage, where the target will be retracted, magnet lifted to beam height, target inserted into polarizing magnet, magnet and microwaves turned on until the target reaches maximum polarization, and the data taking stage, where the magnet and microwaves will be turned off, holding coil turned on, target retracted from the magnet, magnet lowered and then target fully inserted into CLAS.

The target material needs to meet several criteria to be useful in the proposed experiment: it should have a large number of polarizable nuclei, produce high polarization and have long spin relaxation times. The absence of polarized background is also important since the GDH measurement determines the spin dependence of the total photoabsorption cross section. We propose to use chemically doped butanol target ($\text{C}_4\text{H}_9\text{OH}$), since the

residual carbon and oxygen are spinless particles. Deuterated butanol can be used as the polarized deuteron target, by replacing protons (H) with deuterons (2H). The polarization levels expected in a 5 Tesla magnetic field at temperatures of a few 100 mK can exceed 95% for protons with hold times of around 200 hours, and 65% for deuterons with longer hold hours. The characteristics of the Hall B tagged photon beam define the geometry of the target cell. The target diameter is 15 mm which is a minimum size compatible with the 12 mm beam spot on the target. The target length is defined by conflicting demands of the high count rate and cooling requirements. The target length has been optimized through simulation of photonuclear processes in the target, and was found to be about 50 mm. [31] Some parameters of butanol are listed in Table 2.2.

Table 1: Parameters of the Frozen Spin Butanol Target

Chemical Structure	$C_4H_9(OH)$
Target Diameter	15 mm
Target Length	50 mm
Density	0.985 g/cm^3
Dilution Factor	10/74
Packing Factor	~ 0.62

In order to determine the effective dilution factor D_{eff} , it will be necessary to collect data on the unpolarized material. We propose to place a carbon target of the same radiation length as the polarized target at a slightly downstream position, and collect data on it simultaneously at 50 % event rate.

The target polarization will be monitored during the run via the NMR system, in the field of the holding internal solenoid. The calibration of the proton NMR can be done by measurements of polarization in thermal equilibrium, taken with the polarizing magnet. The deuteron signal might be too small for the thermal equilibrium measurement, so we propose to monitor the deuteron polarization through the ratio of the two peaks of the NMR signal (R-ratio method [30]).

2.3 Start Counter

Photon beam experiments require a 'start counter' close to the target to suppress accidental coincidences in the trigger. The target cryostat and the holding magnet are designed to be compatible with the existing CLAS start counter. The only necessary modification to the standard Hall B equipment will be the shielding of the start counter photomultipliers from the fringe field of the target holding coil.

2.4 Trigger

Two types of trigger configuration can be used to make the experiment sensitive to all-neutral events. One such configuration is the coincidence between the tagger MOR in the endpoint region ($\sim k/E > 0.5$) and hit in the forward electromagnetic calorimeter. In this case the trigger threshold can be set to a value higher than minimum ionizing particle energy. This configuration will allow detection of photons from neutral pion decays, and therefore, detection of forward pion events. Another trigger configuration can be formed by requiring coincidence between the TOF signal and the tagger MOR, which will allow detection of charged particles at all angles.

3 Identification of Hadronic Interactions in the Presence of Electromagnetic Backgrounds

3.1 Hadronic Interactions

A hadronic interaction is characterized by one or more produced hadrons in the final state. We have used the PYTHIA Monte Carlo [25] to generate a large sample of hadronic interactions over the proposed energy range. With over 99.5% (99%) probability, at least one of these hadrons will have a transverse momentum $p_T > 0.05$ GeV ($p_T > 0.1$ GeV). Quite often, the final state will include one or more π^0 mesons, which will be detected as photon pairs, generally with a transverse momentum p_T greater than 0.1 GeV. Occasionally the hadronic final state also includes electrons or positrons from π^0 Dalitz decays or from K^0 decays. The Monte Carlo events allow us to determine the idealized detector efficiency as a function of the maximum and minimum detection angles θ_{min} and θ_{max} , and the minimum energy of the particles p_{min} , with and without the detection of photons/electrons. Ideally, one would have full angular acceptance for the detectors, but in practice this is exceedingly difficult, and in fact not needed because of the forward boost from center of mass (c.m.) to lab system, which increases with energy. The minimum detection angle θ_{min} will be somewhere between 6 and 10 degrees, and while the frozen spin target will allow detection of scattering angles larger than 45 degrees, we used θ_{max} of 45 degrees in the simulation, which is the limiting angle when using a standard polarized target. The acceptance efficiency will be slightly higher in case of the frozen spin target, where the maximum scattering angle is ~ 140 degrees.

About 75% of the average fractional energy of hadronic events emerges in the form of charged pions, nucleons/anti-nucleons, and kaons, and about 25% goes to photons and electrons. A few percent goes to neutrinos, whose energy is not detected at all, and about 1% goes to muons, whose energy is only partially detected. The neutrinos and muons originate from pion and kaon decays.

Using a simplified CLAS acceptance model we plot the hadronic event detection efficiency in Fig.2 for four different p_{min} , with and without the detection of photons. Since the CLAS ϕ acceptance varies with θ , data will have to be weighted with θ . The minimum momentum of detected particles should be 0.3 GeV, with θ_{min} between 6 and 10 degrees,

which can be achieved by taking data with the inbending and outbending torus configurations, and averaging the data. With these conditions and the detection of photons, the efficiencies are on the order of 95%.

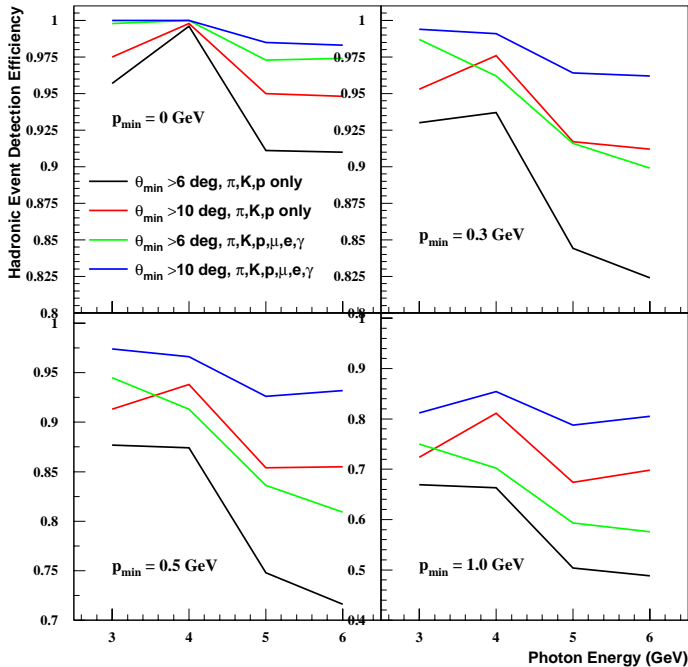


Figure 2: Efficiency for detecting hadronic events with CLAS

3.2 Electromagnetic background

The electromagnetic backgrounds that we wish to reject consist principally of Bethe-Heitler electron/positron elastic and quasi-elastic pair production [22] and Compton scattering from atomic electrons. These reactions occur at low p_T (0.0005 GeV for Bethe Heitler, $\sqrt{0.00025E}$ for atomic Compton), and always have an electron in the final state. Because the target is about 0.1 r.l. and 2.9 barn^{-1} in thickness, and roughly one electron/positron pair is produced per radiation length, compared to a hadronic interaction rate of 10^{-4} per b^{-1} , the Bethe-Heitler rate is about 1000 times larger than the hadronic interaction rate per photon. Fortunately, most of the electron/positron pairs are produced at very small angles (characteristic angle is m_e/k).

The Compton and BH backgrounds can be eliminated by vetoing on electrons and positrons using the electromagnetic calorimeter to separate pions from electrons ($EC/P < 0.24$) and requiring no Cherenkov signal.

A similar rejection mechanism was used by previous experiments [12, 8], where electromagnetic backgrounds were eliminated by rejecting tagged photons for which a forward

angle electron is detected.

4 Expected Results

The quantity of interest $\Delta\sigma^{\gamma N}(k)$ will be determined by measuring the asymmetry in the counting rates $A_1(k)$. The raw helicity asymmetry is

$$A_{raw} = \frac{N_{\uparrow\uparrow} - N_{\uparrow\downarrow}}{N_{\uparrow\uparrow} + N_{\uparrow\downarrow}}, \quad (3)$$

where $N_{\uparrow\uparrow}$, $N_{\uparrow\downarrow}$ are the number of events, corrected for beam charge and dead time, with the beam and target spins parallel and antiparallel respectively. The true asymmetry $A_1(k)$ is determined by dividing the raw asymmetry by the product of target polarization, photon beam polarization and the dilution factor. The error on $A_1(k) = \Delta\sigma^{\gamma N}(k)/2\sigma^{\gamma N}(k)$ is given by

$$\delta A_1(k) = \frac{1}{P_\gamma P_t f \sqrt{N}},$$

where P_γ is the average photon polarization (typically 0.7), P_t is the average target polarization (0.9 for butanol, 0.65 for deuterated butanol), and N is the number of counts. The error on $\Delta\sigma^{\gamma N}(k)$ is simply obtained by scaling the error on $A_1(k)$ by $2\sigma^{\gamma N}(k)$, which is approximately constant at $250 \mu\text{b}$ in our energy range. The dilution factor is approximately $10/74$ for $\text{C}_4\text{H}_9(\text{OH})$, and $20/74$ for $\text{C}_4^2\text{H}_9(\text{O}^2\text{H})$. According to ref. [5, 6], $\Delta\sigma^{\gamma N}(k)$ for the proton is expected to be $\approx 20 \mu\text{b}$ at 4 GeV. A 5 percent uncertainty in $\Delta\sigma^{\gamma N}(k)$ results in $\delta A_1(k)$ of 0.004.

The expected count rate in a kinematic bin width of ΔE is given by

$$Rate = \sigma_{total} \times \Phi \times \frac{\Delta E}{E} \times t_{thickness} \times Acceptance \quad (4)$$

For this calculation, we consider an average cross section on the proton of $\sigma_{total} = 10^{-4}$ barn, based on the predictions of [5]. We consider the photon flux $\Phi = 10^7 \gamma/s$ at the photon energy of $E = 4 \text{ GeV}$, energy bin width of 0.1 GeV. The target thickness $t_{thickness}$ is

$$t_{thickness} = \rho l N_A = 2.97 \text{ barn}^{-1}, \quad (5)$$

where ρ, l are the target density and length, and N_A is Avogadro's number. With these parameters, and assumed CLAS acceptance of 85 %, we estimate the rate of 63.11 Hz per kinematic bin. The number of counts needed to achieve desired error $\delta A_1(k)$ is N .

$$\begin{aligned} \delta A_1(k) = 0.004 &= \frac{1}{\sqrt{N} f P_\gamma P_t} \\ N &= \left(\frac{2\sigma}{\Delta\sigma} \frac{1}{f P_\gamma P_t} \right)^2, \end{aligned} \quad (6)$$

where f is the dilution factor of $10/74$, and $P_\gamma P_t$ is the product of target and beam polarization. The time required to accumulate this statistics is

$$Time = N/Rate \quad (7)$$

Assuming the average photon polarization of 60%, average proton polarization in the frozen spin target of 80%, and a reasonable goal of relative error of 5%, we estimate the required time of approximately 60 hours. In order to accumulate good statistics with both the in-bending and outbending torus configurations, the required time will be approximately 100 hours, or 5 days.

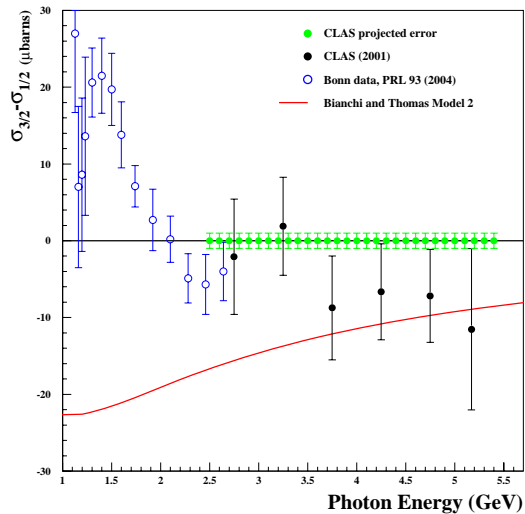


Figure 3: Recent results on $\Delta\sigma^{\gamma p}(k)$ from Bonn [38], a test run in CLAS [34], and the projected statistical error bars for the proposed experiment on polarized protons. Please note that the sign convention used in this plot follows the convention of Bonn-Mainz experiments and is opposite to that of Eq. 1 and Fig. 1.

A similar measurement on the deuterated target will require roughly twice the time needed for the proton measurement.

We estimated the event rate of ~ 63 Hz per energy bin of 0.1 GeV. Assuming 30 such bins in the photon energy range of $2.5 < k < 5.5$, the total event rate will be ~ 1.9 Hz. Given the maximum CLAS DAQ rate of 3.5 kHz, it might be possible to increase the photon flux up to $\Phi = 2 \times 10^7 \gamma/s$. The estimated statistical error bars are plotted in Fig. 3, along with the recent results from Bonn [38], and results from the short CLAS test run [34]. The systematic errors will consist of errors in determination of the target and beam polarization, target dilution factor, photon flux determination, and additional uncertainties in counting of hadronic events. Based on previous experiments, we expect the combined error from determination of polarization and dilution factors to be on the order of 5-7%. The uncertainty in the photon flux determination is on the order of $\sim 2\%$. The systematic

error will most likely be dominated by uncertainty in hadron counting and bias towards detecting certain reactions over the others. Taking data with the inbending and outbending torus configurations, and different torus current should provide a check on some systematic effects.

We plan to extract $\Delta\sigma^{\gamma N}$ from the data in two ways. In the first method, the difference of rates for the two helicity states is converted to cross sections directly using the measured detector acceptance and target thickness. In the second method, the asymmetry in counting rates will be corrected by a calculated dilution factor, and converted to $\Delta\sigma^{\gamma N}$ using previously measured values of $\sigma^{\gamma N}(k)$. In this method, factors such as the detector efficiency cancel, so that some systematic errors will be reduced (while others will be increased). The expected magnitude of the experimental asymmetries is relatively small, and will likely be less than 0.01. Comparison of the two analysis methods will give a valuable check on the evaluation of systematic errors.

During this run, $\Delta\sigma$ can be studied as a function of minimum scattering angle and momentum in CLAS, with extrapolation to perfect acceptance. Many exclusive reactions, such as π , η , and vector meson photoproduction will also be measured at the same time, providing complementary data for study of strangeness and target single spin asymmetry in these reactions.

5 Request

We request 15 days of running time, with 5 days of data taking with the polarized proton target and 10 days of data taking with the polarized deuteron target. During this time we will take data with the inbending and outbending torus configurations. The experiment will require electron beam current of 5-10 nA, of maximum possible energy. We could successfully take data with electron energy of 5.3 GeV.

References

- [1] S. D. Drell and A. C. Hearn, Phys. Rev. Lett 16, 908 (1966); S. B. Gerasimov, Yad. Fiz. 2, 598 (1966); S.J. Brodsky and J.R. Primack, Ann. Phys. 52 (1969) 315.
- [2] L. Tiator, D. Drechsel, and S.S. Kamalov, <http://arXiv.org/abs/nucl-th/000561> and references therein; <http://arXiv.org/abs/hep-ph/0008306>.
- [3] J. D. Bjorken, Phys. Rev. 148 (1966) 1467; Phys. Rev. D 1 (1970) 1376.
- [4] I. Karliner, Phys. Rev. D7 (1993) 2717; R.L. Workman and R.A. Randt, Phys. Rev. D45 (1992) 1789; A.M. Sandorfi, C.S. Whisnant, and M. Khandaker, Phys. Rev. D50 (1994) R6681; R.A. Randt, I.I. Strakovsky, R.L. Workman, Phys. Rev. C53 (1996) 440; D. Drechsel, G. Klein, Phys. Rev. D58 (1998) 116609.
- [5] N. Bianchi, E. Thomas, Phys. Lett. B 450 (1999) 439; E. Thomas, N. Bianchi, Nucl. Phys. Proc. Suppl. 82 (2000) 256.

- [6] S.D. Bass and M.M. Brisudova, Eur. Phys. J. A4 (1999) 251; S.D. Bass, Mod. Phys. Lett. A12 (1997) 1051 and references therein.
- [7] P.V. Landshoff and S.D. Bass, Phys. Lett. B336 (1994) 537; Close and Roberts, Phys. Lett. B336 (1994) 257.
- [8] For a review, see talks from each laboratory presented at the GDH2000 conference, June 2000, Mainz, Germany. Proceedings to be published by World Scientific (ed. Dieter Drechsel).
- [9] H. Arenhovel, nucl-th/0006083 (GDH2000 conference, June 2000, Mainz, Germany).
- [10] F. M. Steffens *et al.*, Phys. Lett. B447 (1999) 233.
- [11] SLAC E155, P.L. Anthony *et al.*, Phys. Lett. B463 (1999) 339; O. A. Rondon, Phys. Rev. C60 (1999) 035201.
- [12] D.O. Caldwell *et al.*, Phys. Rev. D7 (1973) 1362.
- [13] W. Kaune *et al.*, Phys. Rev. D 11, 478 (1975).
- [14] R. Schwitters, SLAC-TN-70-32 (1970).
- [15] G. Miller and D. Walz, SLAC-PUB-1297.
- [16] D. Luckey and R. Schwitters, Nucl. Instrum. Meth. 81, 164 (1970).
- [17] G. Diambrini Palazzi, Rev. Mod. Phys. 40, 611 (1968).
- [18] R. Jones, <http://zeus.phys.uconn.edu/halld/cobrems-7-97/>
- [19] R. F. Mozley and J. DeWire, Nuovo Cimento 27, 1281 (1983).
- [20] I. M. Nadzhafov, Bulletin of the Academy of Sciences of the USSR, Physical Series Vol 14, No. 10, p. 2248 (1976).
- [21] H. A. Tolhoek, Rev. Mod. Phys. 28 (1956) 277.
- [22] Y.S. Tsai, Rev. Mod. Phys. 46 (1974) 815; 49 (1977) 421 (E).
- [23] T.D. Averett *et al.*, Nucl. Instrum. Meth.A 427 (1999) 440.
- [24] SLAC E154, K. Abe *et al.*, Phys. Rev. Lett. 79 (1997) 26.
- [25] T. Sjostrand, Computer Physics Commun. 82, 74 (1994).
- [26] T. Gehrman, M. Stratmann, Phys. Rev. D56 (1997) 5839.
- [27] E155 Collaboration, P.L. Anthony *et al.*, Phys. Lett. B458 (1999) 536.

- [28] Ch. Bradke *et al.*, Nucl. Instr. and Meth. A 436 (1999) 430
- [29] C. Keith, Presentation at the June 2005 European Workshop on Solid Polarized Targets.
- [30] C. Dulya *et al.*, Nucl. Instr. and Meth. A 354 (1995) 249
- [31] E-03-105: Pion Photoproduction from a Polarized Target
- [32] H.Olsen and L.C.Maximon, Phys. Rev. 114 (1959) 887
- [33] J.Ball, E.Pasyuk, CLAS-NOTE 2005-002
- [34] D.I.Sober, L.Todor, P.E.Bosted, and S.E.Kuhn, in “Proceedings of GDH2002, Genova, July 2002”, M. Anghinolfi, M. Battalieri and R.DeVita, eds., World Scientific (2003), p.253; D.I.Sober *et al.*, in “Proceedings of NSTAR2002, Pittsburgh, October 2002”, S.A.Dytman and E.S.Swanson, eds., World Scientific (2003), p. 353
- [35] E-91-015: Helicity Structure of Pion Photoproduction
- [36] K. Helbing, in “Proceedings of GDH2004 ,Norfolk, June 2004”, S.Kuhn and J-P.Chen eds.
- [37] O. Jahn, in “Proceedings of GDH2004 ,Norfolk, June 2004”, S.Kuhn and J-P.Chen eds.
- [38] H. Dutz *et al.*, Phys. Rev. Lett. 93, 032003 (2004)
- [39] Particle Data Group; D. E. Groom *et al.*, Eur. Phys. J. C 15, 1 (2000)